



ORIGINAL ARTICLE

Facile preparation and properties of superhydrophobic nanocellulose membrane



Guoqing Liu^{a,*}, Chenlu Ji^a, Jing Li^{b,c}, Xiangjun Pan^a

^a College of Chemical and Material Engineering, Quzhou University, Quzhou, Zhejiang 324000, China

^b College of Chemical and Biological Engineering, Zhejiang University, Hangzhou, Zhejiang 310027, China

^c Institute of Zhejiang University-Quzhou, Quzhou, Zhejiang 324000, China

Received 24 March 2022; accepted 15 May 2022

Available online 20 May 2022

KEYWORDS

1H,1H,2H,2H-perfluorooctyl trimethoxysilane;
Ethyl orthosilicate;
Superhydrophobicity;
Nanocellulose membrane

Abstract Superhydrophobic nanocellulose membrane was prepared by synergistically modifying biodegradable nanocellulose with low-carbon perfluoroorganosiloxane and ethyl orthosilicate. The effects of four kinds of low-carbon perfluoroorganosiloxanes with different structures and their ratio to ethyl orthosilicate on the hydrophobic properties of nanocellulose membrane were investigated, and then FT-IR, XPS, XRD, SEM, TEM, AFM, TG and contact angle goniometer were used to characterize the structure and hydrophobic properties of nanocellulose membrane before and after modification. It is found that when the molar ratio of 1H,1H,2H,2H-perfluorooctyltrimethoxysilane (PFOTMS) to ethyl orthosilicate (TEOS) is 1, the modified nanocellulose membrane PFOTMS-TEOS-CNF is loaded with silica nanoparticles both inside and on its surface, and a micro-nano hierarchical rough morphology with low surface energy is constructed. At this point, the root-mean-square roughness (Rq) of nanocellulose membrane is 112 nm, and the static contact angle of water droplet is 153.5°, successfully realizing superhydrophobicity. In addition, compared to unmodified nanocellulose membrane, PFOTMS-TEOS-CNF with better thermal stability includes an additional maximum weight loss rate temperature (491.2 °C). The above advantages markedly improve the shortcomings of pristine nanocellulose, such as superhydrophilicity and insufficient thermal stability, and also broadens its high-value application in many fields.

© 2022 The Author(s). Published by Elsevier B.V. on behalf of King Saud University. This is an open access article under the CC BY-NC-ND license (<http://creativecommons.org/licenses/by-nc-nd/4.0/>).

1. Introduction

The development and application of renewable biomass resources is of great significance to green and sustainable chemistry. Cellulose, as the most abundant, green and renewable biomass resource in nature, can be treated by physical and chemical processes to obtain nanocellulose with higher application value (Panchal et al., 2019; Kim et al., 2015). Compared with cellulose, nanocellulose has wider applications due to its nano-size effect, high elastic modulus, high mechanical strength, biocompatibility, regeneration, and degradability (Panchal et al., 2019; Kim et al., 2015; Jonoobi et al., 2015; Liu et al., 2018; Xie et al., 2019).

* Corresponding author at: College of Chemical and Material Engineering, Quzhou University, Quzhou, Zhejiang 324000, China.

E-mail address: liuguoqingmr@126.com (G. Liu).

Peer review under responsibility of King Saud University.



In recent years, a series of novel nanocellulose-based composites with excellent properties have been developed in the fields of polymer materials (Li et al., 2020; Spinella et al., 2015; Xu et al., 2013; Xu et al., 2013), biomedicine (Dai and Si, 2019; Si and Xu, 2020; Jorfi and Foster, 2015; Si, 2019; Yang and Cranston, 2014), oil–water separation (Yang and Cranston, 2014; Bashar et al., 2017), and electronic devices (Kafy et al., 2016; Sadasivuni et al., 2015; Wang et al., 2016; Wang and Huang, 2021). However, nanocellulose has strong hydrophilic properties due to a large number of hydroxyl groups inherent in the structure, which largely limits its application in many practical fields. Therefore, to solve the problems, superhydrophobic modification of nanocellulose is necessary. Moreover, two conditions must be met to realize this purpose of superhydrophobicity (Wang and Jiang, 2007; Song and Rojas, 2013), one is the construction of a micro-nano rough surface structure, which is mainly based on the Wenzel and Cassie-Baxter model theory (Wenzel, 1936; Cassie and Baxter, 1944), and the other is the decrease of surface energy (Cheng et al., 2015).

At present, the research on nanocellulose-based superhydrophobic materials mainly includes three categories (Sun et al., 2021), nanocellulose-based superhydrophobic coatings (Tang et al., 2021; Liu et al., 2016), nanocellulose-based superhydrophobic membranes (Li et al., 2021; Zhang et al., 2019), and nanocellulose-based superhydrophobic aerogels (Hasan et al., 2019; Zuo et al., 2019; Chen et al., 2020). Among them, nanocellulose-based superhydrophobic membranes have recently attracted increasing attention and have become a research hotspot, and two kinds of methods have been developed for preparing the superhydrophobic membranes (Li et al., 2021; Wang et al., 2020; Shi et al., 2019; Ioannis et al., 2015; Baidya et al., 2017; Musikavanhu et al., 2019; Pegah et al., 2018). The first method is using organosilane compounds such as (1H,1H,2H,2H-perfluorodecyltrimethoxysilane, 1H,1H,2H,2H-perfluorodecyltrichlorosilane) to chemically modify nanocellulose, and then getting superhydrophobic nanocellulose membrane by spraying or vacuum filtration. However, C8 perfluorocompounds (including $-(CF_2)_7CF_3$) involved in this method are difficult to degrade in the environment and have been completely banned internationally. Another method is by mixing nanocellulose with functionalized nanoparticles to build a rough surface structure to enhance the hydrophobicity of the membrane, and then by impregnating, spraying or chemical vapor deposition to graft low surface energy silane compounds onto the surface of the membrane to achieve superhydrophobicity. However, the complex preparation process, high equipment and environmental protection requirements greatly limit the popularization and application of the above two methods. Therefore, it is highly necessary to develop a simple, green and efficient method for the preparation of nanocellulose-based superhydrophobic membrane.

In this work, a facile method for the preparation of nanocellulose-based superhydrophobic membrane was developed. Nanocellulose emulsion was used as starting material, and low-carbon perfluoroorganosiloxane was used as modification reagent to reduce the surface energy, with simultaneous addition of ethyl orthosilicate for prehydrolysis. The modified nanocellulose mixed solution was prepared by a one-pot method, and then the superhydrophobic nanocellulose membrane was obtained by vacuum filtration, drying and solidification.

2. Experimental section

2.1. Reagents

Nanocellulose emulsion (CNF, 1 wt%) was purchased from Jinjiahao green nanomaterials Co., Ltd.; 1H,1H,2H,2H-perfluorooctyltrimethoxysilane (PFOTMS, 97%), (1,1,2,2-Tetrahydroxynonafluorohexyl)trimethoxysilane (NFHTMS, $\geq 97\%$), trimethoxy(pentafluorophenyl)silane (PFPTMS, $\geq 97\%$), 3,3,3-(trifluoropropyl)trimethoxysilane (TFPTMS, $\geq 96\%$) and ethyl orthosilicate (TEOS, 99.99%) were purchased from

Shanghai Macklin biochemical technology Co., Ltd.; glacial acetic acid (AR) was purchased from Xilong scientific company.

2.2. Preparation of superhydrophobic nanocellulose membrane

30 mL of nanocellulose (CNF) emulsion was added to a three-necked flask with a condenser and a thermometer, and then the emulsion was heated up to 60 °C under vigorous stirring. Afterwards, 2 mmol of low-carbon perfluoroorganosiloxane and a certain amount of ethyl orthosilicate were added dropwise, and glacial acetic acid was added to adjust the pH value (until pH = 4). After reacting for 6 h, the mixture was cooled to room temperature, and then a certain amount of the resultant mixture was poured into a sand core funnel for the vacuum filtration, and then a wet nanocellulose membrane was obtained. Finally, the wet membrane was placed in an oven at 100 °C for 24 h to get the superhydrophobic nanocellulose membrane. The schematic diagram of PFOTMS-TEOS-CNF membrane fabrication was shown in Scheme 1.

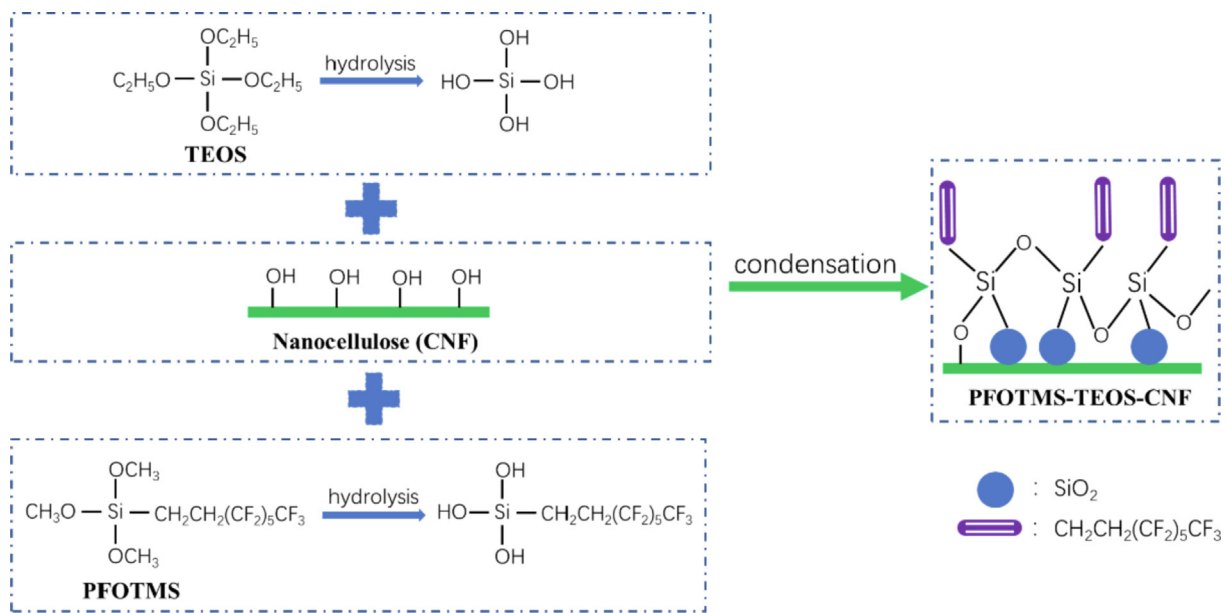
2.3. Characterization of samples

Fourier transform infrared spectroscopy (FTIR) of samples were recorded using an infrared spectrometer (Nicolet Is50, Thermo Fisher Scientific Co., Ltd.) in the wavenumber range of 4000–400 cm^{-1} ; The surface morphology of membranes were observed using a field emission scanning electron microscope (SU8010, Japan Hitachi Co., Ltd.) with the extra-high-tension (EHT) of 5.00 kV, while the samples were sputtered with a layer of Au before observation; Water contact angle (WCA) of membranes were measured using a contact angle goniometer (DSA30S, Kruss Scientific Instrument Co., Ltd.) with the deionized water droplet volume of 2 μL ; The pyrolysis behaviors of samples were tested using a thermogravimetric analyzer (TGA2, Mettler-Toledo, Switzerland) with the temperature range of 30–600 °C at a heating rate of 10 °C/min under nitrogen atmosphere; Scanning within a 2θ range of 5–70°, X-ray diffraction patterns were obtained using an X-ray diffractometer (XRD-6100, Shimadzu, Japan) at a voltage of 40 kV, a current of 30 mA and a scan speed of 5°/min using Cu K α radiation ($\lambda = 0.154178 \text{ nm}$); The surface chemical composition and chemical bonding information of membranes were obtained by using a X-ray photoelectron spectrometer (K-Alpha, Thermo Fisher Scientific); The surface roughness of membranes were measured with a tapping mode by using a atomic force microscope (SPM-9700, Shimadzu, Japan); The micromorphology of cross section of the membranes were observed using a transmission electron microscope (JEM-2100F, JEOL, Japan) with an acceleration voltage of 200 kV, while the samples were pretreated by using ultrathin-section method before observation.

3. Results and discussion

3.1. Optimization of the selection of low-carbon perfluoroorganosiloxane

According to the preparation method of 2.2, four kinds of low-carbon perfluoroorganosiloxanes (PFOTMS, NFHTMS,



PFPTMS and TFPTMS) were used to modify nanocelluloses to prepare four membranes without adding ethyl orthosilicate and glacial acetic acid, which were denoted as PFOTMS-CNF, NFHTMS-CNF, PFPTMS-CNF and TFPTMS-CNF, respectively. Contact angle goniometer and scanning electron microscope were used to investigate the water contact angle and surface microstructure of the samples, and the results are shown in Figs. 1 and 2, respectively. It is found that PFOTMS-CNF and PFPTMS-CNF display good hydrophobic properties with water contact angles of 132.2° and 126.6° , respectively, which mainly results from the existence of cross-linking between PFOTMS/PFPTMS and nanocellulose to make the formation of compact membrane (as shown in SEM images). At the same time, the introduction of fluorine-containing groups reduces the surface energy of membrane (Cardellini et al., 2021; Joseph and Ellen, 2021). As for NFHTMS-CNF and TFPTMS-CNF, the water contact angles are respectively 89.8° and 15.3° , and the surfaces are hydrophi-

lic. Moreover, it can be seen from Fig. 2c–e that the surface structure of the modified samples is almost unchanged compared with that of CNF. Therefore, considering cost and performance, PFOTMS is finally determined to be the modification monomer.

3.2. Optimization of TEOS:PFOTMS molar ratio

According to the preparation method of 2.2, a series of hydrophobic nanocellulose membrane samples (PFOTMS-TEOS-CNF) were prepared by using PFOTMS as modification reagent, and the molar ratio of TEOS to PFOTMS was optimized. The static contact angle of water droplets and the macroscopic state of the surface of membrane were observed, and the results are shown in Table 1. The photographs and contact angle test pictures of samples are shown in Fig. 3. It is found that, when $n(\text{TEOS:PFOTMS}) < 1$, the water contact angle of the modified nanocellulose membrane gradually increases with the increasing amount of TEOS. When $n(\text{TEOS:PFOTMS}) = 1$, the modified nanocellulose membrane displays superhydrophobic property with a water contact angle of 153.5° , at which the surface of the sample is smooth. When $n(\text{TEOS:PFOTMS}) = 1.25$, the water contact angle is 156.9° , and the membrane still maintains superhydrophobic property, but the surface of the membrane is rough with some bulges. When $n(\text{TEOS:PFOTMS}) = 1.5$, the water contact angle is decreased to 143.4° , and the surface is rough and peeled off. Therefore, the generated silica will not be fully loaded on the nanocellulose with excess amount of TEOS, and the excess silica would cause bulge or falling off. So the molar ratio of TEOS to PFOTMS was determined to be 1, and all the PFOTMS-TEOS-CNF membranes in the following paragraphs refer to samples prepared under such condition.

3.3. IR spectra analysis

Infrared spectroscopy was used to characterize and analyze the changes of functional groups before and after modification of

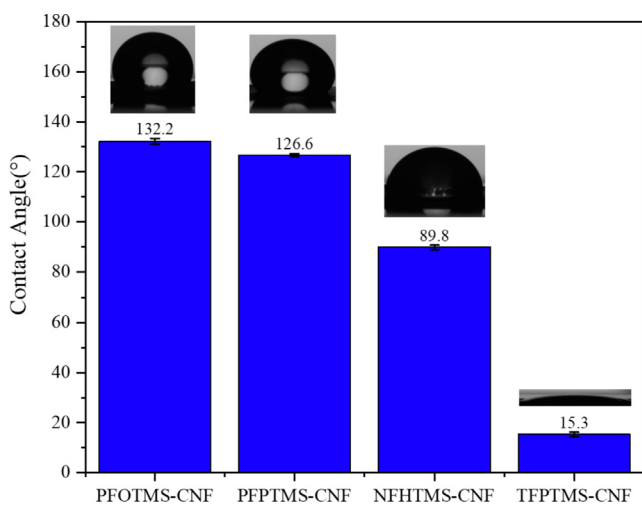


Fig. 1 Contact angles of the prepared samples.

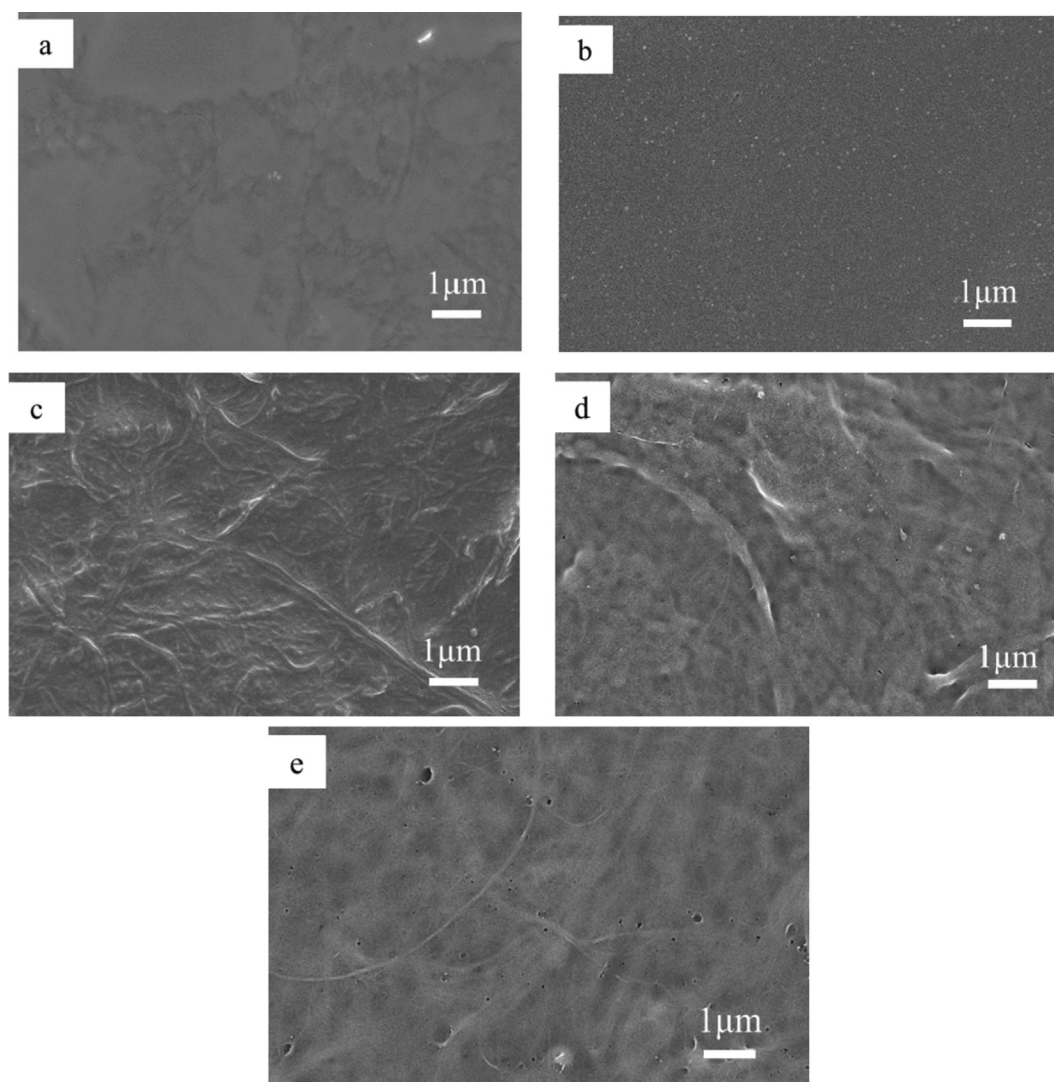


Fig. 2 SEM images of (a) PFOTMS-CNF, (b) PFPTMS-CNF, (c) NFHTMS-CNF, (d) TFPTMS-CNF, (e) CNF.

Table 1 Variation of the contact angle and surface macroscopic state of the membranes with the molar ratio of n (TEOS: PFOTMS).

n (TEOS: PFOTMS)	Contact angle ($^{\circ}$)	Macroscopic State
0	132.2 ± 1.0	Smooth
0.75	145.3 ± 0.5	Smooth
1	153.5 ± 0.6	Smooth
1.25	156.9 ± 1.6	Rough and bulged
1.5	143.4 ± 2.1	Rough and peeled off

the nanocellulose membrane (Fig. 4). It can be seen that the spectra have obvious differences, the characteristic absorption peak of nanocellulose at 3335 cm^{-1} for the O—H stretching vibration is significantly weakened after modification, indicating that most O—H groups of nanocellulose has undergone the modification reaction. The C—O—C stretching vibration absorption peak of the nanocellulose at 1034 cm^{-1} shows a blue shift after modification (Zuo et al., 2019), that is because the introduction of electron-withdrawing perfluorinated

groups has reduced the electron density of the nanocellulose skeleton structure. Moreover, the characteristic absorption peaks in the range of $1034\text{--}1545\text{ cm}^{-1}$ are partially overlapped before and after modification. The absorption peaks of CNF are mainly attributed to the stretching vibrations of C—OH and C—C and the bending vibrations of O—H and C—H (Le et al., 2016), while the absorption peak of modified CNF is attributed to the stretching vibration of CF_2 , CF_3 , Si—O—Si (Zuo et al., 2019; Gao et al., 2020; Jiang et al., 2021). Besides, the newly added characteristic peaks in the range of $560\text{--}804\text{ cm}^{-1}$ and the characteristic peak at 436 cm^{-1} are assigned to silica, which are mainly attributed to the stretching vibration of Si—C and Si—O—C (Le et al., 2016; Gao et al., 2020; Jiang et al., 2021). Therefore, these results verify that a chemical modification reaction occurs between PFOTMS, TEOS and CNF.

3.4. XPS analysis

X-ray photoelectron spectroscopy (XPS) was used to characterize the surface element composition of the nanocellulose

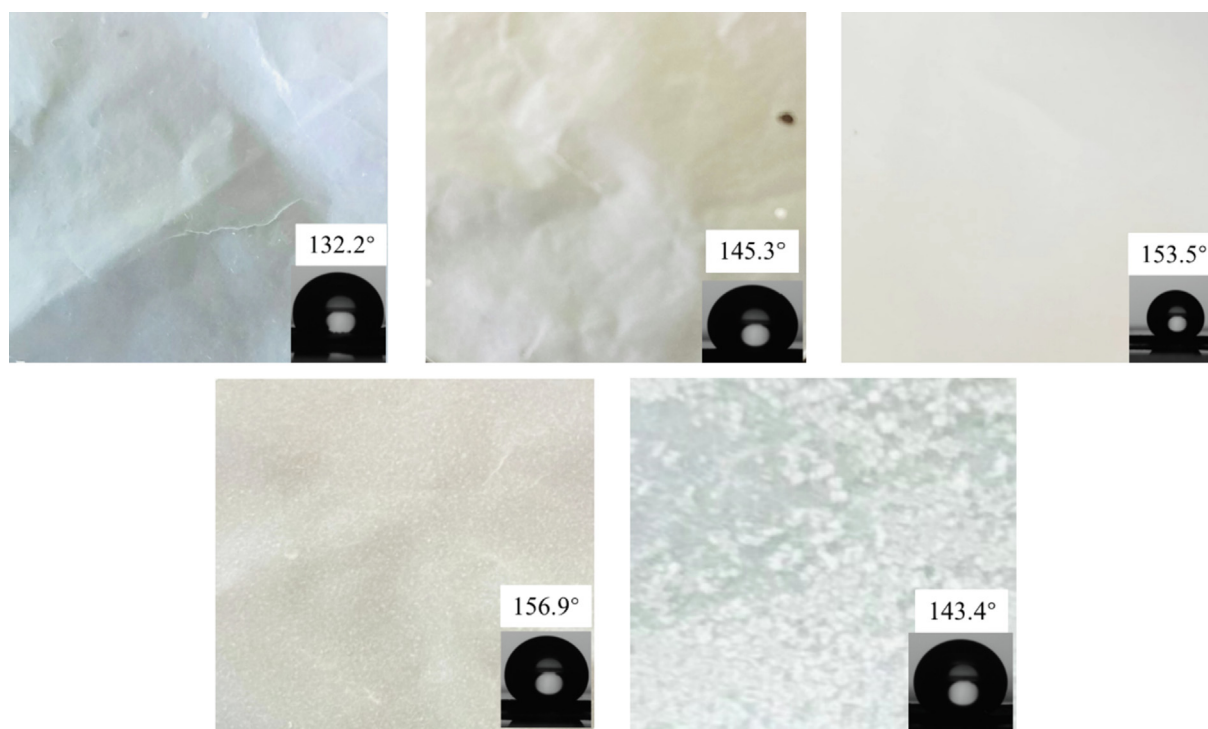


Fig. 3 Photographs and contact angle test pictures of samples, (Note: inset 132.2° contact angle test picture is a duplication of inset in Fig. 1.).

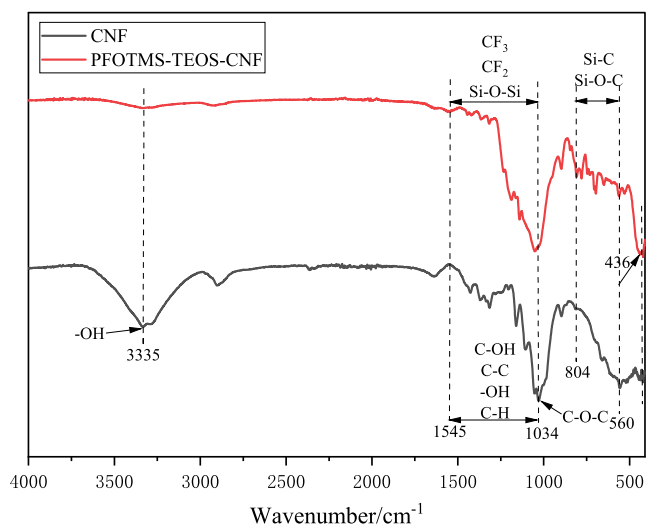


Fig. 4 IR spectra of CNF and PFOTMS-TEOS-CNF.

membranes before and after modification. Fig. 5a shows the XPS survey spectra of CNF and PFOTMS-TEOS-CNF, in addition to C 1s and O 1s characteristic peaks, the characteristic peaks of F 1s, Si 2s, and Si 2p are observed at the binding energies of 689, 154, and 102 eV, respectively, indicating that the incorporation of F and Si elements for the PFOTMS-TEOS-CNF. Fig. 5b, c, and d show the high-resolution XPS spectra of F 1s, Si 2p, and C 1s of PFOTMS-TEOS-CNF, respectively. Fig. 5c displays the peaks at 102.8, 102.1, and 101.5 eV, corresponding to Si—O, C—Si—O, and Si—C, respectively. The five characteristic peaks at 294.3, 292.0, 288.3,

286.8, and 285.6 eV in Fig. 5d are assigned to CF₃, CF₂, O—C—O, C—O, and C—C/C—H/C—Si (Piłkowski et al., 2021; Giner et al., 2019; Chen et al., 2021), respectively. The above results further demonstrate the successful modification of PFOTMS and TEOS for nanocellulose.

3.5. XRD analysis

X-ray diffraction was used to characterize and analyze the changes in the crystal phase structure of the nanocellulose membrane (CNF) before and after modification (Fig. 6). It can be seen that the CNF has the characteristic diffraction peaks at $2\theta = 15.0, 16.5, 18.5$ and 23.0° . And the modified PFOTMS-TEOS-CNF has a new characteristic diffraction peak at $2\theta = 26.6^\circ$, which is assigned to (422) facet of crystalline silica. While the characteristic diffraction peaks at $2\theta = 15.0^\circ, 16.5^\circ$ basically disappear and the characteristic diffraction peaks at $2\theta = 18.5^\circ, 23.0^\circ$ obviously weaken, indicating that the crystallinity of the modified PFOTMS-TEOS-CNF significantly decreases, which is caused by the formation and incorporation of crystalline silica and cross-linking reaction between PFOTMS/TEOS and nanocellulose. All above destroy the crystal structure of nanocellulose to some extent and reduce its lattice order degree.

3.6. SEM and TEM analysis

Scanning electron microscopy was used to characterize and analyze the changes in the surface microstructure of the nanocellulose membranes before and after modification (Fig. 7). Fig. 7a and b are the SEM images of the original nanocellulose membrane, which displays a nanofibrillar struc-

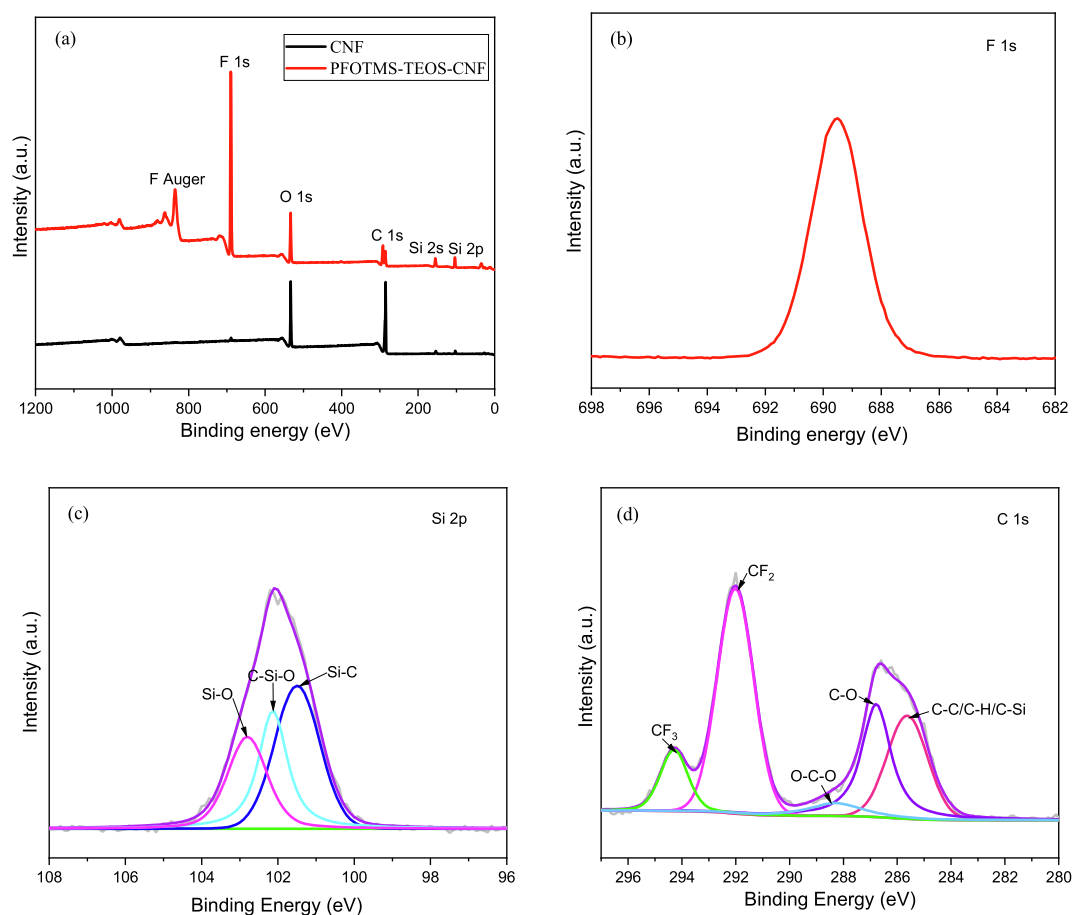


Fig. 5 (a) XPS survey spectra of the prepared samples, high-resolution XPS spectra of (b) F 1s, (c) Si 2p and (d) C 1s.

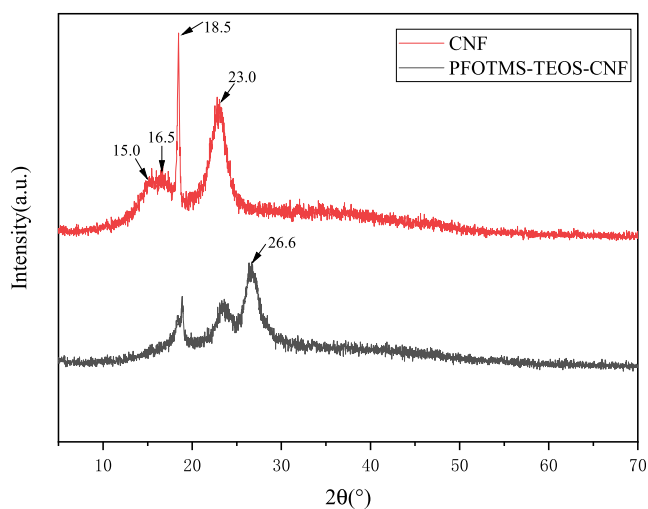


Fig. 6 XRD patterns of CNF and PFOTMS-TEOS-CNF.

ture, a relatively smooth surface, and a small number of nanopores. Fig. 6c and d show the SEM images of the modified PFOTMS-TEOS-CNF membrane, it is found that the PFOTMS-TEOS-CNF has a more obvious network structure formed by interweaving of nanofibrils. There are a large number of nanopores in the framework, and a large number of

stacked silica nanoparticles evenly load on the surface, thereby a porous hierarchical structure with a good micro-nano rough surface is constructed. After modification, the surface morphology of the membrane changes from the Wenzel model state to the Cassie-Baxter model state, and the surface hydrophobicity is significantly improved, as shown in Fig. 8.

The micromorphology of cross section of the superhydrophobic PFOTMS-TEOS-CNF membrane was characterized by TEM, while the sample was pretreated by using ultrathin-section method before observation. The results are shown in Fig. 9. It is found that the modified PFOTMS-TEOS-CNF still retains the network structure of nanofibers, and the fibers of PFOTMS-TEOS-CNF are decorated with a large number of tiny silica nanoparticles. So combined with the SEM results, it can be concluded that the modified nanocellulose membrane PFOTMS-TEOS-CNF is loaded with silica nanoparticles both inside and on its surface.

3.7. AFM analysis

Surface roughness is one of the most important factors affecting the hydrophobicity of the membrane. Atomic force microscopy was used to characterize and analyze the surface roughness of PFOTMS-TEOS-CNF, PFOTMS-CNF, and CNF membranes, as shown in Fig. 10. The root-mean-square roughness (R_q) of PFOTMS-TEOS-CNF surface with superhydrophobicity is 112 nm, and the water contact angle is

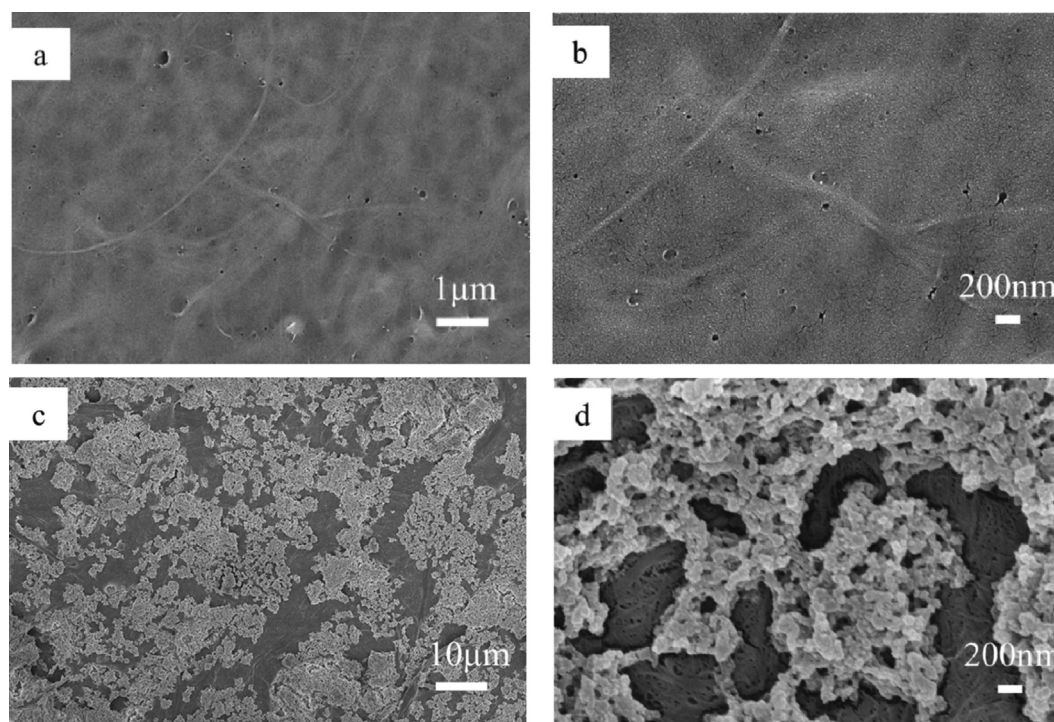


Fig. 7 SEM images of (a, b) CNF and (c, d) PFOTMS-TEOS-CNF. (Note: (b) is a zoom of central area of (a). (d) is a zoom of central area of (c). (a) is a duplication of Fig. 2e.).

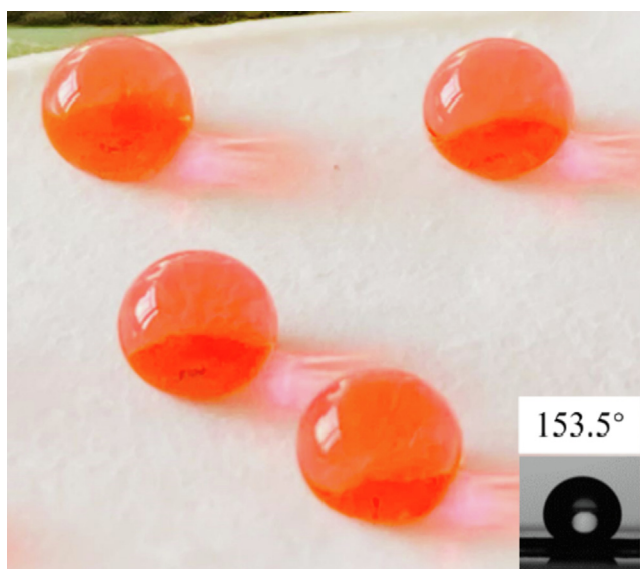


Fig. 8 Image of superhydrophobicity and contact angle test of PFOTMS-TEOS-CNF. (Note: inset 153.5° contact angle test picture is a duplication of inset in Fig. 3.).

153.5°. The root-mean-square roughness (R_q) of PFOTMS-CNF with hydrophobicity is 10 nm, and the water contact angle is 132.2°. The root-mean-square roughness (R_q) of the unmodified CNF is 45 nm, and it is highly wettable with the water contact angle of 13.3°. The surface roughness order of the three samples is: PFOTMS-TEOS-CNF > CNF > PFOT

MS-CNF, which is consistent with the SEM images. Above results show that PFOTMS-CNF modified by single PFOTMS has good hydrophobicity because of its low surface energy, but the roughness is not enough to achieve superhydrophobicity. However, PFOTMS-TEOS-CNF modified by PFOTMS and TEOS both have low surface energy and good roughness, so its superhydrophobic performance is achieved.

3.8. TG analysis

Thermogravimetric analyzer was used to characterize the thermal stability of the nanocellulose membrane before and after modification, Fig. 11a and b are the TG and DTG curves, respectively. It can be seen that with the increase of temperature, CNF undergoes a rapid thermal decomposition weight loss process at 240 °C, and the maximum weight loss rate occurs at 339.5 °C, and then it tends to slow thermal decomposition after 390 °C. The same phenomenon is observed in the temperature range of 240–390 °C for PFOTMS-TEOS-CNF, which indicates that thermal weight loss at this stage mainly results from the decomposition of a small amount of unmodified CNF (Le et al., 2016; Abraham et al., 2011; Liu et al., 2016). Combined with the DTG results, the thermal behavior of the modified PFOTMS-TEOS-CNF has undergone significant changes with two maximum weight loss rate temperatures: 339.5 and 491.2 °C, and also it is found that the rapid thermal decomposition process still occurs after 390 °C. The thermal stability of PFOTMS-TEOS-CNF is significantly improved, which further indicates that most of the hydroxyl groups on the nanocellulose are modified to form a certain degree of chemical cross-linking.

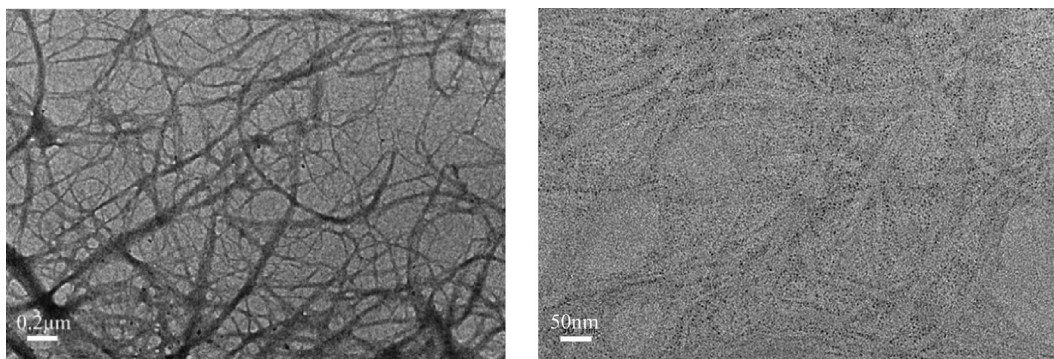


Fig. 9 TEM images of PFOTMS-TEOS-CNF.

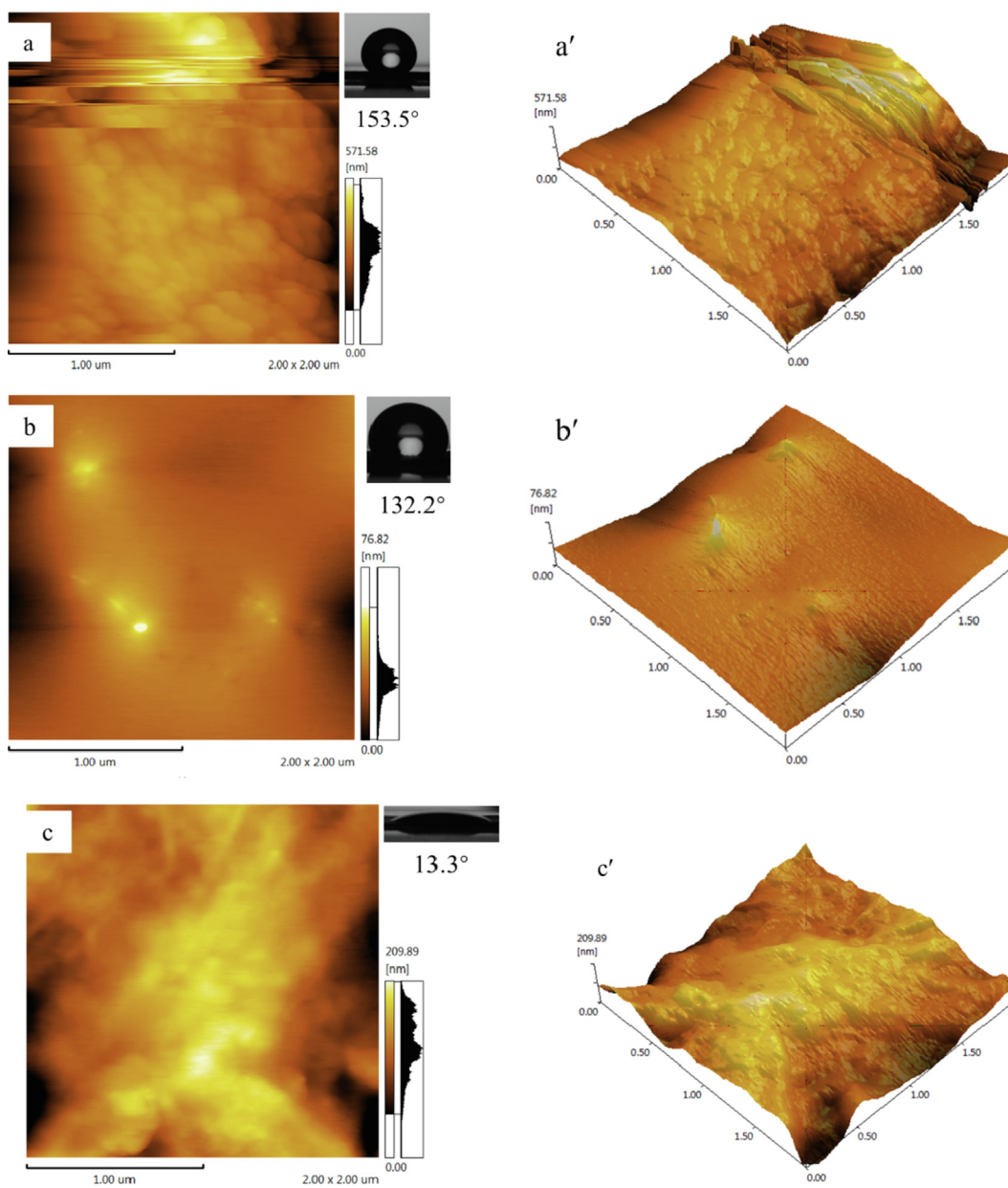


Fig. 10 2D and 3D AFM images of (a/a') PFOTMS-TEOS-CNF, (b/b') PFOTMS-CNF and (c/c') CNF. (Note: insets 153.5° and 132.2° contact angle test pictures are duplications of inset in Fig. 3 and Fig. 1 respectively.)

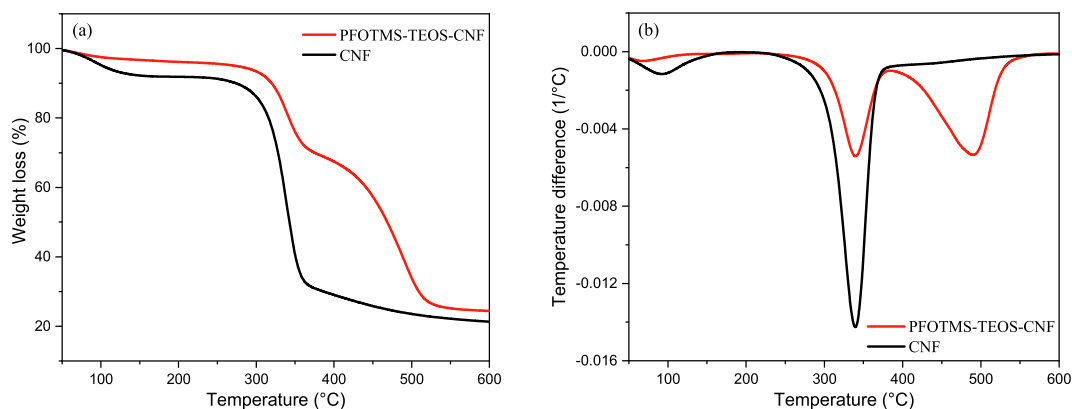


Fig. 11 (a) TG and (b) DTG curves of CNF and PFOTMS-TEOS-CNF.

4. Conclusions

In conclusion, the superhydrophobic nanocellulose membrane was successfully prepared by using both low-carbon perfluoroorganosiloxane and ethyl orthosilicate as modification reagents with a one-pot method. PFOTMS was screened as the low-carbon perfluoroorganosiloxane modification monomer. When the molar ratio of TEOS to PFOTMS is 1, the water contact angle of the prepared modified nanocellulose membrane PFOTMS-TEOS-CNF reaches 153.5°, and superhydrophobic property is achieved. The modified nanocellulose membrane PFOTMS-TEOS-CNF retains the crystalline network structure of nanocellulose and loads a large amount of silica nanoparticles both inside and on its surface. In the work, PFOTMS is responsible for the decrease of surface energy, and TEOS is responsible for formation of silica nanoparticles to construct a micro-nano rough surface structure, which synergistically create the typical rough surface with low surface energy to obtain superhydrophobicity, while the water droplet is in a Cassie-Baxter state on the membrane surface. Furthermore, PFOTMS-TEOS-CNF displays better thermal stability compared with CNF. The prepared superhydrophobic nanocellulose membrane is a promising candidate for the superhydrophobic environmental protection composite materials, which will greatly expand its potential applications in the areas of self-cleaning, energy storage, and waterproof packaging materials.

Declaration of Competing Interest

The authors declare that they have no known competing financial interests or personal relationships that could have appeared to influence the work reported in this paper.

Acknowledgements

This work was supported by Basic Public Welfare Research Project of Zhejiang Province (LGG21B060001), and Science and Technology Project of Institute of Zhejiang University-Quzhou (IZQ2019-KJ-026).

References

- Abraham, E., Deepa, B., Pothan, L.A., Jacob, M., Thomas, S., Cvelbar, U., Anandjiwala, R., 2011. Extraction of nanocellulose fibrils from lignocellulosic fibres: A novel approach. *Carbohydr. Polym.* 86, 1468–1475.
- Baidya, A., Ganayee, M.A., Jakka Ravindran, S., Tam, K.C., Das, S. K., Ras, R.H.A., Pradeep, T., 2017. Organic solvent-free fabrication of durable and multifunctional superhydrophobic paper from waterborne fluorinated cellulose nanofiber building blocks. *ACS Nano* 11 (11), 11091–11099.
- Bashar, M.M., Zhu, H., Yamamoto, S., Mitsuishi, M., 2017. Superhydrophobic surfaces with fluorinated cellulose nanofiber assemblies for oil-water separation. *RSC Adv.* 7, 37168–37174.
- Cardellini, A., Bellussi, F.M., Rossi, E., Chiavarini, L., Becker, C., Cant, D., Asinari, P., Sebastiani, M., 2021. Integrated molecular dynamics and experimental approach to characterize low-free-energy perfluoro-decyl-acrylate (PFDA) coated silicon. *Mate. Design* 208, 109902.
- Cassie, A.B.D., Baxter, S., 1944. Wettability of porous surfaces. *Trans. Faraday Soc.* 40, 546–550.
- Chen, I.H., Wei You, M., Tsai, J.H., Chang, J.H., Cheng, I.C., Hsu, C. C., Luo, S.C., Chen, C.F., Chen, J.Z., 2021. Feasibility Study of Dielectric Barrier Discharge Jet-Patterned Perfluorodecyl-trichlorosilane-Coated Paper for Biochemical Diagnosis. *ECS J. Solid State SC.* 10, 037005.
- Chen, J.Q., Yu, Y., Shang, Q.Q., Han, J.G., Liu, C.G., 2020. Enhanced Oil Adsorption and Nano-Emulsion Separation of Nanofibrous Aerogels by Coordination of Pomelo Peel-Derived Biochar. *Ind. Eng. Chem. Res.* 59 (18), 8825–8835.
- Cheng, M.J., Song, M.M., Dong, H.Y., Shi, F., 2015. Surface adhesive forces: A metric describing the drag-reducing effects of superhydrophobic coatings. *Small* 11, 1665–1671.
- Dai, L., Si, C.L., 2019. Recent advances on cellulose-based nano-drug delivery systems: design of prodrugs and nanoparticles. *Curr. Med. Chem.* 26 (14), 2410–2429.
- Gao, M.Q., Zhang, H., Chen, T.T., Fan, L., Wen, Y.B., Liu, P.T., Liu, Z., 2020. Preparation and characterization of hydrophobic cellulose nanofibril aerogels. *J. Funct. Mater.* 51 (2), 02107–02112.
- Giner, I., Torun, B., Han, Y., Duderija, B., Meinderink, D., Orive, A. G., Arcos, T., Weinberger, C., Tiemann, M., Schmid, H.J., Grundmeier, G., 2019. Water adsorption and capillary bridge formation on silica micro-particle layers modified with perfluorinated organosilane monolayers. *Appl. Surf. Sci.* 475, 873–879.
- Hasan, M., Deepu, A.G., Vishnu, A., Yasir, B.P., Sisanth, K.S., Daniel, P., Matej, B., Bastien, S., Ange, N., Sabu, T., Samsul, R., Abdul Khalil, H.P.S., 2019. Robust Superhydrophobic Cellulose Nanofiber Aerogel for Multifunctional Environmental Applications. *Polymers* 11 (3), 495.
- Ioannis, K., Diana, G., Dimitra, A., Katerina, E.A., 2015. Facile Method to Prepare Superhydrophobic and Water Repellent Cellulosic Paper. *J. Nanomater.*, 219013
- Jiang, S.J., Zhou, S.S., Du, B., Luo, R.B., 2021. Preparation of the Temperature-Responsive Superhydrophobic Paper with High Stability. *ACS Omega* 6, 16016–16028.
- Jonoobi, M., Oladi, R., Davoudpour, Y., Oksman, K., Dufresne, A., Hamzeh, Y., Davoodi, R., 2015. Different preparation methods

- and properties of nanostructured cellulose from various natural resources and residues: A review. *Cellulose* 22, 935–969.
- Jorfi, M., Foster, E.J., 2015. Recent advances in nanocellulose for biomedical applications. *J. Appl. Polym. Sci.* 132 (14), 41719.
- Joseph, A.J., Ellen, M.S., 2021. Recent advances in the preparation of semifluorinated polymers. *Polym. Chem.* 12 (45), 6515–6526.
- Kafy, A., Akther, A., Shishir, M.I.R., Kim, H.C., Yun, Y.M., Kim, J., 2016. Cellulose nanocrystal/graphene oxide composite film as humidity sensor. *Sens. Actuat. A-Phys.* 247, 221–226.
- Kim, J.H., Shim, B.S., Kim, H.S., Lee, Y.J., Min, S.K., Jang, D., Abas, Z., Kim, J., 2015. Review of Nanocellulose for Sustainable Future Materials. *Int. J. Pr. Eng. Man-gt.* 2, 197–213.
- Le, D., Kongparakul, S., Samart, C., Phanthong, P., Karnjanakom, S., Abudula, A., Guan, G.Q., 2016. Preparing hydrophobic nanocellulose-silica film by a facile one-pot method. *Carbohydr. Polym.* 153, 266–274.
- Li, Y.F., Chen, C.J., Song, J.W., Yang, C.P., Kuang, Y.D., Vellore, A., Hitz, E., Zhu, M.W., Jiang, F., Yao, Y.G., Gong, A., Martini, A., Hu, L.B., 2020. Strong and Superhydrophobic Wood with Aligned Cellulose Nanofibers as a Waterproof Structural Material. *Chinese J. Chem.* 38 (8), 823–829.
- Li, A.L., Wang, G.F., Zhang, Y., Zhang, J.Q., He, W.J., Ren, S.Y., Xu, Z.H., Wang, J.W., Ma, Y.W., 2021. Preparation methods and research progress of superhydrophobic paper. *Coordin. Chem. Rev.* 449, 214207.
- Liu, R., Dai, L., Si, C.L., 2018. Mussel-inspired cellulose-based nanocomposite fibers for adsorption and photocatalytic degradation. *ACS Sustain. Chem. Eng.* 6 (11), 15756–15763.
- Liu, H., Gao, S.W., Cai, J.S., He, C.L., Mao, J.J., Zhu, T.X., Chen, Z., Huang, J.Y., Meng, K., Zhang, K.Q., Al-Deyab, S.S., Lai, Y.K., 2016. Recent Progress in Fabrication and Applications of Superhydrophobic Coating on Cellulose-Based Substrates. *Materials* 9 (3), 124.
- Liu, D.D., Tang, Y.J., Zhang, X.Q., Huang, B.B., Zhang, W.Q., 2016. Preparation, modification and its application of nanocrystalline cellulose in barrier coating of cellulosic paper. *J. Funct. Mater.* 10 (47), 10239–10244.
- Musikavanhu, B., Hu, Z.J., Dzapata, R.L., Xu, Y.C., Christie, P., Guo, D.L., Li, J., 2019. Facile method for the preparation of superhydrophobic cellulosic paper. *Appl. Surf. Sci.* 496, 143648.
- Panchal, P., Ogunsona, E., Mekonnen, T., 2019. Trends in advanced functional material applications of nanocellulose. *Processes* 7 (1), 10.
- Pegah, K., Alistair, W.T.K., Gabriel, J.P., Leena-Sisko, J., Mauri, A. K., Robin, H.A.R., 2018. Superhydrophobic paper from nanostructured fluorinated cellulose esters. *ACS Appl. Mater. Inter.* 10 (13), 11280–11288.
- Pilkowski, M., Morgiante, G., Mysliwiec, J., Kuchowicz, M., Marczak, J., 2021. Environmental testing of hydrophobic fluorosilane-modified substrates. *Surf. Interfaces* 23.
- Sadasivuni, K.K., Kafy, A., Zhai, L.D., Ko, H.U., Mun, S., Kim, J., 2015. Transparent and Flexible Cellulose Nanocrystal/Reduced Graphene Oxide Film for Proximity Sensing. *Small* 11 (8), 994–1002.
- Shi, C.C., Wu, Z.H., Xu, J.F., Wu, Q.Q., Li, D.J., Chen, G.X., He, M. H., Tian, J.F., 2019. Fabrication of transparent and superhydrophobic nanopaper via coating hybrid SiO₂/MWCNTs composite. *Carbohydr. Polym.* 225, 11522.
- Si, C.L., 2019. The development of lignocellulosic biomass in medicinal applications. *Curr. Med. Chem.* 26 (14), 2408–2409.
- Si, C.L., Xu, J.Y., 2020. Recent advances in bio-medicinal and pharmaceutical applications of bio-based materials. *Curr. Med. Chem.* 27 (28), 4581–4583.
- Song, J.J., Rojas, O.J., 2013. Approaching super-hydrophobicity from cellulosic materials: A Review. *Nord. Pulp Pap. Res. J.* 28 (2), 216–238.
- Spinella, S., Re, G.L., Liu, B., Dorgan, J., Habibi, Y., Leclère, P., Raquez, J.M., Dubois, P., Gross, R.A., 2015. Polylactide/cellulose nanocrystal nanocomposites: Efficient routes for nanofiber modification and effects of nanofiber chemistry on PLA reinforcement. *Polymer* 65, 9–17.
- Sun, L., Zhang, X.Y., Liu, H.Y., Liu, K., Du, H.S., Kumar, A., Sharma, G., Si, C.L., 2021. Recent Advances in Hydrophobic Modification of Nanocellulose. *Cur. Org. Chem.* 25 (3), 417–436.
- Tang, X.Y., Huang, W., Xie, Y.J., Xiao, Z.F., Wang, H.G., Liang, D. X., Li, J., Wang, Y.G., 2021. Superhydrophobic Hierarchical Structures from Self-Assembly of Cellulose-Based Nanoparticles. *ACS Sustain. Chem. Eng.* 9, 14101–14111.
- Wang, Y., Huang, J.T., 2021. Transparent, conductive and superhydrophobic cellulose films for flexible electrode application. *RSC Adv.* 11, 36607–36616.
- Wang, S., Jiang, L., 2007. Definition of superhydrophobic states. *Adv. Mater.* 19 (21), 3423–3424.
- Wang, Q., Xie, D., Chen, J.J., Liu, G., Yu, M.G., 2020. Superhydrophobic paper fabricated via nanostructured titanium dioxide-functionalized wood cellulose fibers. *J. Mater. Sci.* 55, 7084–7094.
- Wang, S.M., Zhang, X.X., Wu, X.D., Lu, C.H., 2016. Tailoring percolating conductive networks of natural rubber composites for flexible strain sensors via a cellulose nanocrystal templated assembly. *Soft Matter* 12, 845–852.
- Wenzel, R.N., 1936. Resistance of solid surfaces to wetting by water. *Ind. Eng. Chem.* 28 (8), 988–994.
- Xie, H.X., Zou, Z.F., Du, H.S., Zhang, X.Y., Wang, X.M., Yang, X. H., Wang, H., Li, G.B., Li, L., Si, C.L., 2019. Preparation of thermally stable and surface-functionalized cellulose nanocrystals via mixed H₂SO₄/Oxalic acid hydrolysis. *Carbohydr. Polym.* 223, 115116.
- Xu, S.H., Girouard, N., Schueneman, G., Shofner, M.L., Meredith, J. C., 2013. Mechanical and thermal properties of waterborne epoxy composites containing cellulose nanocrystals. *Polymer* 54 (24), 6589–6598.
- Xu, X.Z., Liu, F., Jiang, L., Zhu, J.Y., Haagensohn, D., Wiesenborn, D.P., 2013. Cellulose Nanocrystals vs. Cellulose Nanofibrils: A Comparative Study on Their Microstructures and Effects as Polymer Reinforcing Agents. *ACS Appl. Mater. Inter.* 5, 2999–3009.
- Yang, X., Cranston, E.D., 2014. Chemically cross-linked cellulose nanocrystal aerogels with shape recovery and superabsorbent properties. *Chem. Mater.* 26, 6016–6025.
- Zhang, S., Li, W., Wang, W., Wang, S.F., Qin, C.R., 2019. Reactive superhydrophobic paper from one-step spray-coating of cellulose-based derivative. *Appl. Surf. Sci.* 497, 143816.
- Zuo, K.M., Wu, J.J., Chen, S.Q., Ji, X.X., Wu, W.B., 2019. Superamphiphobic nanocellulose aerogels loaded with silica nanoparticles. *Cellulose* 26, 9661–9671.